

Title: Phenology and diversity in Zambia

Authors: Godlee J. L.¹, Ryan C. M.¹, Siampale A.², Dexter K. G.^{1,3}

¹School of GeoSciences, University of Edinburgh, Edinburgh, United Kingdom

²Forestry Department Headquarters - Ministry of Lands and Natural Resources, Cairo Road, Lusaka, Zambia

³Royal Botanic Garden Edinburgh, Edinburgh, EH3 5LR, United Kingdom

Corresponding author:

John L. Godlee

johngodlee@gmail.com

School of GeoSciences, University of Edinburgh, Edinburgh, United Kingdom

Acknowledgements

Author contribution statement

JLG conceived the study, conducted the analysis, and wrote the first draft of the manuscript. AS coordinated plot data collection in Zambia, and initial data management. All authors contributed to manuscript revisions.

Data accessibility statement

The data used in this study are held by the Zambian Integrated Land Use Assessment Project (ILUA-II), and were cleaned by the SEOSAW project (Socio-Ecological Observatory for Southern African Woodlands). An anonymised version of the plot data are available at the following DOI: .

Abstract

1 Introduction

The seasonal timing and duration of foliage production (land-surface phenology) is a key mediator of land-atmosphere exchanges. Foliage forms the primary interface between plants, the atmosphere and sunlight (Gu et al., 2003; Penuelas et al., 2009), thus land-surface phenology plays an important role in regulating global carbon, water and nitrogen cycles (Richardson et al., 2013). Carbon-cycling models routinely incorporate land-surface phenological processes, most commonly through remotely-sensed data products (e.g. Bloom et al. 2016), but our understanding of the ecological mechanisms which determine these phenological processes remains under-developed (Whitley et al., 2017). This limits our ability to predict how land-surface phenology will respond to climate and biodiversity change, and how these responses will vary among species and vegetation types (Xia et al., 2015).

At regional scales, land-surface phenology can be predicted using only climatic factors, namely precipitation, diurnal temperature, and light environment (Adole et al., 2018b), but significant local variation exists within biomes in the timing of leaf production which cannot be attributed solely to abiotic environment (Stöckli et al., 2011). It has been repeatedly suggested that the diversity and composition of plant species plays a role in determining how ecosystems respond to abiotic phenological cues (Adole et al., 2018a; Jeganathan et al., 2014; Fuller, 1999), owing to differences in life history strategy among species and demographic groups, but current implementation of biotic variation in carbon cycling models is often limited to coarse plant functional types, which are unable to represent the wide variation in phenological patterns observed at local scales (Scheiter et al., 2013; Pavlick et al., 2013).

Across the dry tropics, seasonal oscillations in water availability produce strong cycles of foliage production (Chidumayo, 2001; Dahlin et al., 2016), with knock-on effects for ecosystem function. The phenomenon of pre-rain green-up seen in some tree species within the dry tropics serves as a striking example of adaptation to seasonal variation in water availability (Ryan et al., 2017). Conservative species, i.e. slower growing, with robust leaves and denser wood, may initiate leaf production (green-up) before the rainy season has commenced. More acquisitive species and juveniles however, tend to green-up during the rainy season creating a dense leaf-flush during the mid-season peak of growth and dropping their leaves earlier as the wet season ends. Both strategies have associated costs and benefits which allow species exhibiting a range of phenological syndromes along this spectrum to co-exist. While conservative species gain a competitive advantage from having fully emerged leaves when the rainy season starts, they must also invest heavily in deep root architecture to access dry season groundwater reserves in order to produce foliage during the dry season. Similarly, while

34 acquisitive species minimise the risk of hydraulic failure and mortality by only producing leaves when
35 conditions are amenable, they forfeit growing season length. It has been suggested that variation
36 in phenological strategy among tree species is one mechanism by which increased species diversity
37 increases resilience to drought and maximises productivity in water-limited woodland ecosystems
38 (Stan & Sanchez-Azofeifa, 2019; Morellato et al., 2016). By providing functional redundancy within
39 the ecosystem, leaf production can be maintained under a wider range of conditions, therefore
40 maximising long-term productivity.

41 In addition to determining productivity, variation in leaf phenology also affects broader ecosystem
42 function. Woodlands with a longer tree growth period support a greater diversity and abundance of
43 wildlife, particularly birds, but also browsing mammals and invertebrates (Cole et al., 2015; Araujo
44 et al., 2017; Morellato et al., 2016; Ogutu et al., 2013). As climate change increases the frequency and
45 severity of drought in water-limited woodlands, it is feared that this will result in severe negative
46 consequences for biodiversity (Bale et al., 2002). The periods of green-up and senescence which
47 bookend the growing season are key times for invertebrate reproduction (Prather et al., 2012) and
48 herbivore browsing activity (Velasque & Del-Claro, 2016; Morellato et al., 2016). Pre-rain green-up
49 provides a valuable source of moisture and nutrients before the rainy season, and can moderate
50 the understorey microclimate, increasing humidity, reducing UV exposure, and moderating diurnal
51 oscillations in temperature, reducing ecophysiological stress which can lead to mortality during the
52 dry season. Additionally, a slower rate of green-up caused by tree species greening at different times,
53 i.e. reduced synchronicity, provides an extended period of bud-burst, maintaining the important food
54 source of nutrient rich young leaves for longer. Thus, understanding the determinants of seasonal
55 patterns of tree leaf production in dry deciduous woodlands can provide valuable information on
56 spatial variation in vulnerability to climate change, and help to model their contribution to land
57 surface carbon cycle models under climate change.

58 In this study we investigated how tree species diversity, composition, and demographic structure
59 influence three key measurable aspects of the tree phenological cycle of dry tropical woodlands:
60 (1) the lag time between green-up/senescence and the start/end of the rainy season, (2) the rates
61 of greening and senescence at the start and end of the seasonal growth phase, and (3) the overall
62 length of the growth period. It is hypothesised that: (H_1) due to variation among species in minimum
63 viable water availability for growth, sites with greater tree species richness will exhibit slower rates of
64 greening and senescence as different species green-up and senesce at different times. We hypothesise
65 that: (H_2) in sites with greater species richness the start of the growing season will occur earlier
66 with respect to the onset of rain due to an increased likelihood of containing a species which can
67 green-up early. We hypothesise that: (H_3) sites with greater species richness will exhibit a longer
68 growth period and greater cumulative green-ness over the course of the growth period, due to a higher

69 resilience to variation in water availability. We hypothesise that: (H₄) irrespective of species diversity,
70 variation in tree species composition and vegetation type will cause variation in the phenological
71 metrics outlined above. Finally, we hypothesise that: (H₅) within vegetation types, sites with larger
72 trees will exhibit earlier pre-rain green-up, under the assumption that large trees can better access
73 deep groundwater reserves ahead of seasonal rainfall.

74 2 Materials and methods

75 2.1 Plot data

76 We used plot-level data on tree species diversity and composition across 672 sites from the Zambian
77 Integrated Land Use Assessment Phase II (ILUA-II), conducted in 2014 (Mukosha & Siampale,
78 2009; Pelletier et al., 2018). Each site consisted of four 20x50 m (0.1 ha) plots positioned in a square
79 around a central point, with a distance of 500 m between each plot (Figure 2). The original census
80 contained 993 sites, which was filtered in order to define study bounds and to ensure data quality.
81 Only sites with ≥ 50 stems ha⁻¹ ≥ 10 cm DBH (Diameter at Breast Height) were included in the
82 analysis, to ensure all sites represented woodlands rather than ‘grassy savanna’, which is considered
83 a separate biome with different species composition and ecosystem processes governing phenology
84 (Parr et al., 2014). Sites dominated by non-native tree species ($\geq 50\%$ of individuals), e.g. *Pinus*
85 spp. and *Eucalyptus* spp. were excluded, as these species may exhibit non-seasonal patterns of
86 foliage production (Broadhead et al., 2003). Of the 56634 trees recorded, 2% were only identified to
87 genus, and 7.7% could not be identified.

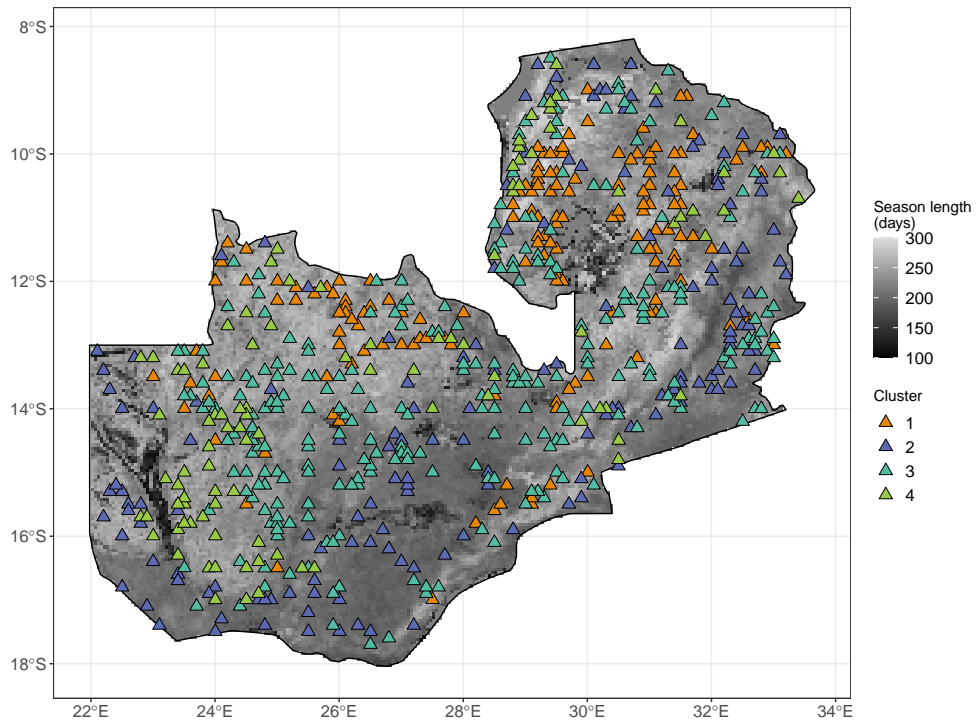


Figure 1: Distribution of study sites within Zambia as triangles, each consisting of four plots. Sites are colored according to vegetation compositional cluster as identified by Ward's clustering algorithm on the Bray-Curtis distance of plots. Zambia is shaded according to growing season length as estimated by the MODIS VIPPHEN-EVI2 product, at 0.05° spatial resolution (Didan & Barreto, 2016).

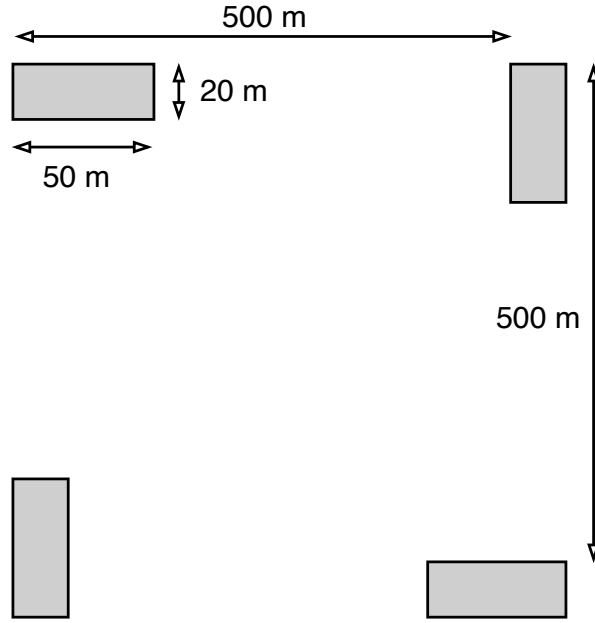


Figure 2: Schematic diagram of plot layout within a site. Each 20x50 m (0.1 ha) plot is shaded grey. The site centre is denoted by a circle. Note that the plot dimensions are not to scale.

88 Within each plot, the species of all trees with at least one stem ≥ 10 cm DBH were recorded. Plot
 89 data was aggregated to the site level for analyses to avoid pseudo-replication caused by the more
 90 spatially coarse phenology data. Tree species composition varied little among the four plots within
 91 a site, and were treated as representative of the woodland in the local area. Using the Bray-Curtis
 92 dissimilarity index of species abundance data (), we calculated that the mean pairwise compositional
 93 distance between plots within a site was lower than the mean compositional distance across all pairs
 94 of plots in 88.4% of cases.

95 2.2 Plot data analysis

96 To measure variation in tree species composition we used agglomerative hierarchical clustering on
 97 species basal area abundance data (Kreft & Jetz, 2010; Fayolle et al., 2014). To guard against
 98 sensitivity to rare individuals, which can preclude meaningful cluster delineation across such a large
 99 species compositional range, we excluded species with less than five records, and to sites with more
 100 than five species. We used Ward's algorithm to define clusters (Murtagh & Legendre, 2014), based
 101 on the Bray-Curtis distance of sites. We determined the optimal number of clusters by maximising
 102 the mean silhouette width among clusters (Rousseeuw, 1987) Figure S3. Vegetation type clusters
 103 were used later as interaction terms in linear models. We described the vegetation types represented
 104 by each of the clusters using a Dufrene-Legendre indicator species analysis (Dufrêne & Legendre,
 105 1997).

106 To describe the species diversity of each site, we calculated the Shannon-Wiener index (H') from
 107 species basal area rather than individual abundance, as a measure of species richness effectively
 108 weighted by a species' contribution to canopy occupancy. H' was then transformed to the first order
 109 numbers-equivalent (1D) of H' , calculated as $e^{H'}$ (Jost, 2007). We use 1D as the primary measure
 110 of species richness in our statistical models and is subsequently referred to as such. Additionally, we
 111 calculated a separate measure of abundance evenness, using the Shannon Equitability index ($E_{H'}$)
 112 (Smith & Wilson, 1996). $E_{H'}$ was calculated as the ratio of basal area Shannon-Wiener diversity
 113 index to the natural log of total basal area per site.

114 To describe average tree size, we calculated the quadratic mean of stem diameters per site (Curtis &
 115 Marshall, 2000). The quadratic mean gives more weight to large trees and is thus more appropriate
 116 for our use, where we are interested in the contribution of large trees to woodland structure. We
 117 also calculated the diversity of tree sizes using the coefficient of variation of stem diameters per site.

118 2.3 Land-surface phenology data

119 To quantify phenology at each site, we used the MODIS MOD13Q1 satellite data product at 250 m
 120 resolution (Didan, 2015). The MOD13Q1 product provides an Enhanced Vegetation Index (EVI)
 121 time series at 16 day intervals. EVI is widely used as a measure of vegetation growth, as an
 122 improvement to NDVI (Normalised Differential Vegetation Index), which tends to saturate at higher
 123 values. Annual cumulative EVI is well-correlated with gross primary productivity and so can act as
 124 a suitable proxy (Sjöström et al., 2011). We used all scenes from January 2010 to December 2020
 125 with less than 20% cloud cover covering the study area. All sites were determined to have a single
 126 annual growth season according to the MODIS VIPPHEN product (Didan & Barreto, 2016), which
 127 assigns pixels (0.05° , 5.55 km at equator) up to three growth seasons per year. We stacked yearly
 128 data between 2010 and 2020 and fit a General Additive Model (GAM) to produce an average EVI
 129 curve. We estimated the start and end of the growing season using first derivatives of the GAM.
 130 Start of the growing season was identified as the first day where the model slope exceeds half of the
 131 maximum positive model slope for a continuous period of 20 or more days, using only backwards
 132 looking data, following White et al. (2009). Similarly, we defined the end of the growing season as
 133 the final day of the latest 20 period where the GAM slope meets or exceeds half of the maximum
 134 negative slope. We estimated the length of the growing season as the number of days between the
 135 start and end of the growing season. We estimated the green-up rate as the slope of a linear model
 136 across EVI values between the start of the growing season and the point at which the slope of
 137 reduces below half of the maximum positive slope. Similarly the senescence rate was estimated as
 138 the slope of a linear model between the latest point where the slope of decrease fell below half of the
 139 maximum negative slope and the end of the growing season Figure 3. We validated our calculations

140 of cumulative EVI, mean annual EVI, growing season length, season start date, season end date,
141 green-up rate and senescence rate with calculations made by the MODIS VIPPHEN product with
142 linear models comparing the two datasets across our study sites (Figure S1, Table S1). We chose
143 not to use the MODIS VIPPHEN product directly due to its more coarse spatial resolution (0.05° ,
144 5.55 km at equator). Sites where our calculation of a phenological metric was drastically different to
145 the MODIS VIPPHEN estimate were excluded, under the assumption that our algorithm had failed
146 to capture the true value or some site specific factor precluded precise estimation. This removed 0
147 sites.

148 Precipitation data was gathered using the “GPM IMERG Final Precipitation L3 1 day V06” dataset,
149 which has a pixel size of 0.1° (11.1 km at the equator) (Huffman et al., 2015), between 2010 and 2020.
150 Daily total precipitation was separated into two periods: precipitation during the growing season
151 (growing season precipitation), and precipitation in the 90 day period before the onset of the growing
152 season (dry season precipitation). Rainy season limits were defined as for the EVI data, using the
153 first derivative of a GAM to create a curve for each site using stacked yearly precipitation data,
154 from which we estimated the half-max positive and negative slope to identify where the GAM model
155 exceeded these slope thresholds for a consistent period of 20 days or more. Mean diurnal temperature
156 range (Diurnal δT) was calculated as the mean of monthly temperature range from the WorldClim
157 database, using the BioClim variables, with a pixel size of 30 arc seconds (926 m at the equator)
158 (Fick & Hijmans, 2017). averaged across all years of available data (1970-2000). We calculated
159 the lag between the onset of the growing season and the onset of the rainy season as the difference
160 between these two dates as calculated above. We performed a similar calculation to estimate the
161 lag between the end of the growing season and the end of the rainy season.

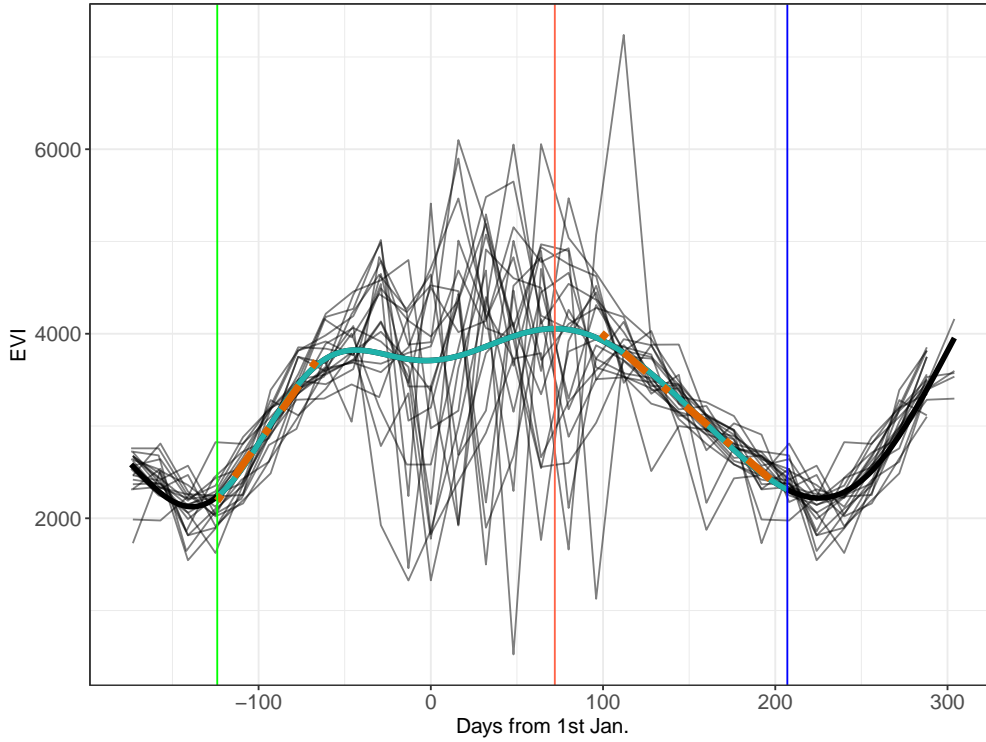


Figure 3: Example EVI time series, demonstrating the metrics derived from it. Thin black lines show the raw EVI time series, with one line for each annual growth season. The thick black line shows the GAM fit. The thin blue lines show the minima which bound the growing season. The red line shows the maximum EVI value reached within the growing season. The shaded cyan area of the GAM fit shows the growing season, as defined by the first derivative of the GAM curve. The two orange dashed lines are linear regressions predicting the green-up rate and senescence rate at the start and end of the growing season, respectively. Note that while the raw EVI time series fluctuate greatly around the middle of the growing season, mostly due to cloud cover, the GAM fit effectively smooths this variation to estimate the average EVI during the mid-season period.

2.3.1 Statistical modelling

We specified multivariate linear models to assess the role of tree species diversity on each of the chosen phenological metrics. We defined a maximal model structure including richness, abundance evenness, the interaction of richness and vegetation type, and climatic variables shown by previous studies to strongly influence phenology. The quality of the maximal model was compared to models with different subsets of independent variables using the model log likelihood, AIC (Akaike Information Criteria), BIC (Bayesian Information Criteria), and adjusted R^2 values for each model. For each phenological metric, the best model according to the model quality statistics is reported in the results. Where two similar models were within 2 AIC points of each other, the model with fewer terms was chosen as the best model, to maximise model parsimony. All models were fitted using

Maximum Likelihood (ML) to allow comparison of models (Zuur et al., 2009). The best model was subsequently re-fitted using Restricted Maximum Likelihood for model effect estimation (REML). Independent variables in each model were transformed to achieve normality where necessary and standardised to Z-scores prior to modelling to allow comparison of slope coefficients within a given model.

To describe variation within and among vegetation types in their land-surface phenology we conducted a principal component analysis of the six phenological metrics we derived from the MOD13Q1 product. We also conducted a simple MANOVA using the phenological metrics as response variables, followed by post-hoc Tukey’s tests between each pairwise combination of vegetation types per phenological metric, to test whether vegetation types differed significantly in their land-surface phenology.

We used the **ggeffects** package to estimate the marginal means of the interaction effect of species diversity and vegetation type, to investigate vegetation type specific effects on each phenological metric (Lüdtke, 2018). Estimated marginal means entails generating model predictions across values of a focal variable, in this case species diversity, while holding non-focal variables constant. All statistical analyses were conducted in R version 4.0.2 (R Core Team, 2020).

3 Results

Model selection showed that richness and evenness are important determinants of each of the chosen phenological metrics, across vegetation types. The effect of richness featured and was significant in all best models except for senescence laf and senescence rate. Evenness was a significant effect in models for cumulative EVI, season length and senescence lag only Figure 4.

3 vegetation type clusters were identified during hierarchical clustering. Cluster 3, which contains the most sites (487), consists of small stature Zambesian woodlands, as referenced by Dinerstein et al. (2017) and Chidumayo (2001), and is not dominated by a particular large canopy tree species. It is possible that these woodlands represent highly disturbed woodlands where large trees may have been removed by humans. Abundance evenness is high across sites in Cluster 3. Cluster 2 is dominated heavily by *Brachystegia boehmii*, while Cluster 1 is dominated by *Julbernardia paniculata*, both large canopy-forming trees. These two clusters likely represent variation among miombo woodland types in dominant canopy tree species. Both Clusters 1 and 2 have a similar composition of non-dominant smaller shrubby species, such as *Pseudolachnostylis maprouneifolia* (Table 1).

As expected (H_3), richness and wet season precipitation both had positive significant effects on cumulative EVI and season length. In contrast, abundance evenness, the other aspect of tree species diversity in our models, had a significant negative effect on both cumulative EVI and season length

205 (Figure 4).

206 Species richness caused a significant increase in the lag time between date of green-up and date of
207 rainy season onset (H_2). This effect was comparable to the effects of pre-season precipitation and
208 diurnal temperature range, which also caused an increase in green-up lag. In contrast, senescence lag
209 was poorly defined by our models, suggesting that some unmeasured factor remains the key driver
210 of this phenological metric. The effects of diurnal δT and abundance evenness had wide confidence
211 interval. The best model explained only 1% of the variance in senescence lag, though was still better
212 quality than a climate-only model.

213 All best models including tree species diversity variables were of better quality than models which
214 included only climatic variables Table 2. The phenological metrics best predicted were green-up
215 lag and cumulative EVI, where models explained 26% and 34% of the variance in these variables,
216 respectively. Senescence rate and senescence lag were the least well predicted phenological metrics,
217 with the best model explaining 3% and 2% of their variance, respectively.

218 While species richness had a significant negative effect on green-up rate, as predicted by H_1 , the best
219 model, which also included pre green-up precipitation and diurnal temperature range, only explained
220 10% of the variance in this metric.

221 The slope of the relationship between species richness and phenological metrics varied among vegeta-
222 tion types, in all models except the model for green-up lag, vegetation types with both positive and
223 negative signs were observed Figure 5. Across all models however, none of the vegetation types were
224 significantly different, according to post-hoc Tukeys's tests on marginal effects (Table S8). Clusters
225 were largely similar in their density distribution of the six phenological metrics Figure 6, and a
226 MANOVA followed by post-hoc Tukey's tests showed no significant differences between any pairwise
227 combination of vegetation types for any phenological metric. The most striking differences are the
228 presence of some sites in Cluster 5 with particularly high green-up rates. The hierarchical clustering
229 analysis demonstrated that there was little spatial structure to the vegetation clusters identified.
230 The key emergent trends were that Clusters 2 and 5 were absent from the southwest of the country
231 (Figure 1) possibly due to the low levels of precipitation in this region, which could preclude many
232 miombo tree species. Additionally Cluster 1 was predominantly restricted to the central western
233 part of the country.

Cluster	N sites	Richness	MAP	Diurnal δT	Species	Indicator value
1	158	16(8)	1173(158.6)	13(1.5)	<i>Brachystegia longifolia</i>	0.397
					<i>Uapaca kirkiana</i>	0.390
					<i>Marquesia macroura</i>	0.285
2	158	13(6)	946(173.8)	14(1.6)	<i>Combretum molle</i>	0.258
					<i>Lannea discolor</i>	0.228
					<i>Combretum zeyheri</i>	0.214
3	257	16(7)	999(160.6)	14(1.5)	<i>Julbernardia paniculata</i>	0.559
					<i>Brachystegia boehmii</i>	0.540
					<i>Pseudolachnostylis maprouneifolia</i>	0.226
4	99	14(6)	1011(183.5)	14(1.7)	<i>Brachystegia spiciformis</i>	0.582
					<i>Cryptosepalum exfoliatum</i>	0.285
					<i>Guibourtia coleosperma</i>	0.281

Table 1: Climatic information and Dufrene-Legendre indicator species analysis for the vegetation type clusters identified by the PAM algorithm, based on basal area weighted species abundances. The three species per cluster with the highest indicator values are shown along with other key statistics for each cluster. MAP (Mean Annual Precipitation) and Diurnal δT are reported as the mean and 1 standard deviation in parentheses. Species richness is reported as the median and the interquartile range in parentheses.

Response	δAIC	δBIC	R^2_{adj}	$\delta \log Lik$
Cumulative EVI	16.3	7.3	0.28	-10.15
Season length	9.1	4.6	0.09	-5.56
Green-up rate	-1.3	-10.3	0.11	-1.36
Senescence rate	2.2	-2.3	0.01	-2.11
Green-up lag	47.2	38.2	0.27	-25.60
Senescence lag	1.6	1.6	0.06	-0.80

Table 2: Model fit statistics for each phenological metric.

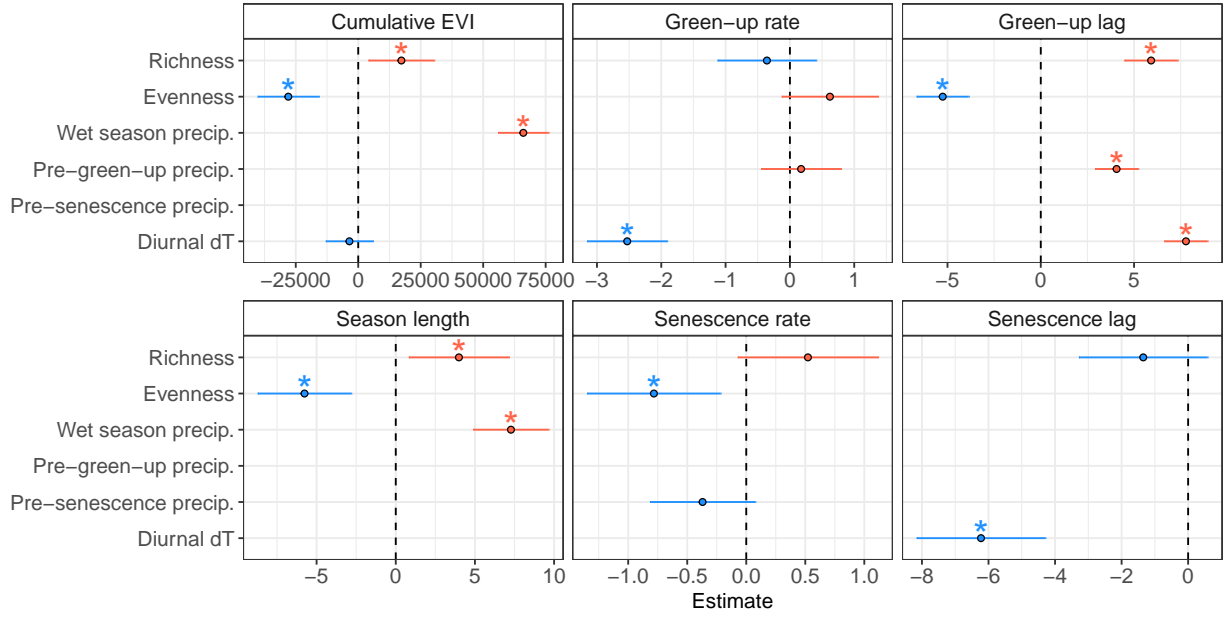


Figure 4: Standardized slope coefficients for each best model of a phenological metric. Slope estimates are ± 1 standard error. Slope estimates where the interval (standard error) does not overlap zero are considered to be significant effects.

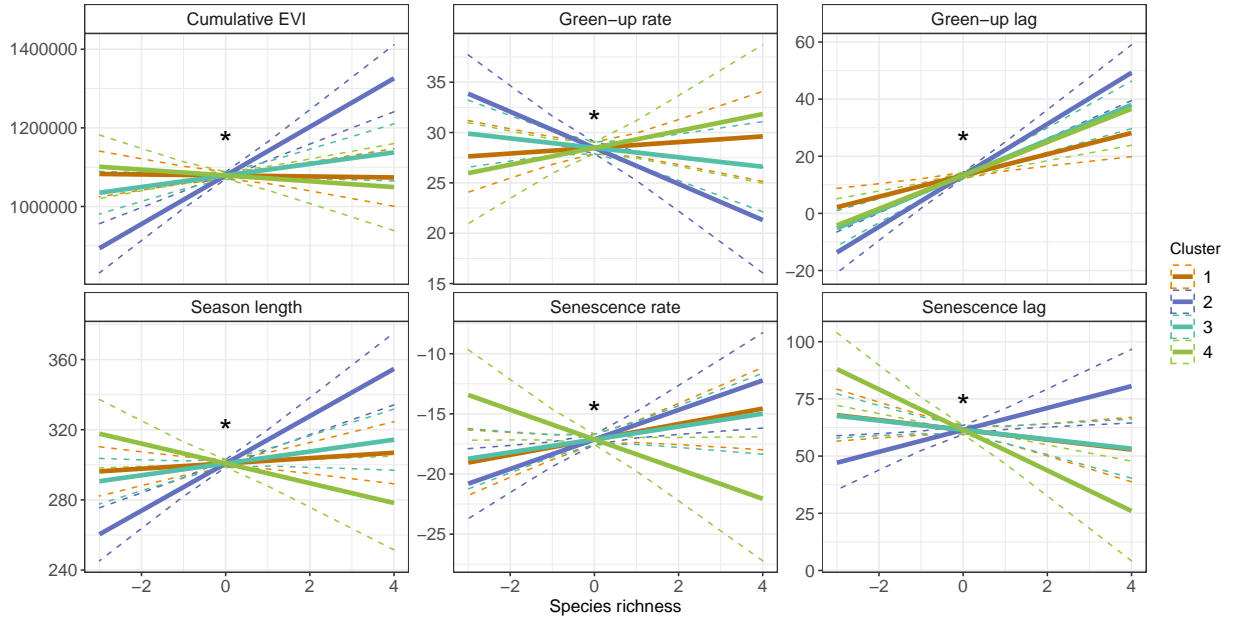


Figure 5: Marginal effects of tree species richness on each of the phenological metrics, for each vegetation type, using the best model including the interaction of species richness and vegetation cluster, for each phenological metric.

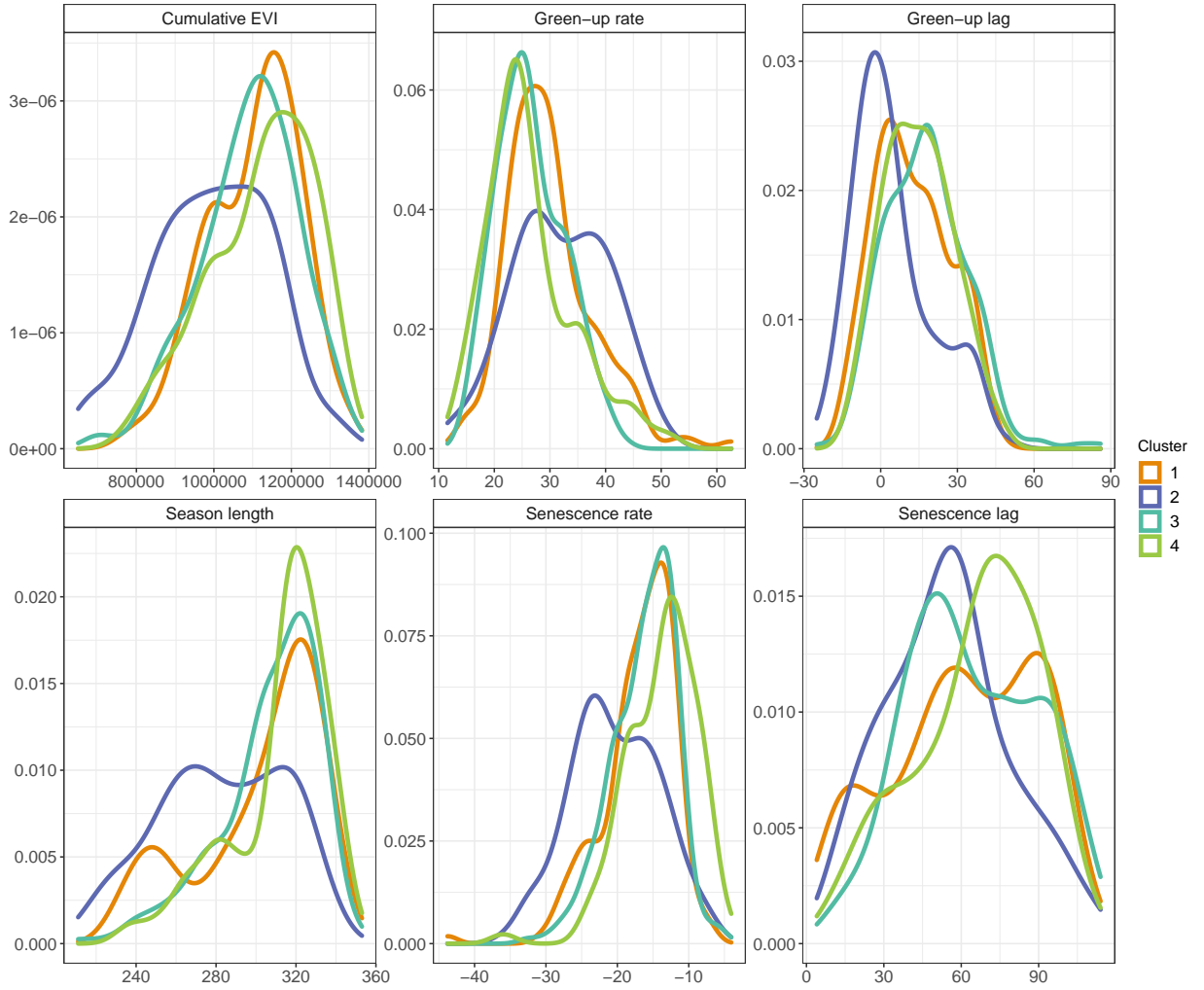


Figure 6: Density distribution of the six phenological metrics used in the study, grouped by vegetation type cluster. For a pairwise comparison of phenological metrics and their correlations, see Figure S2.

4 Discussion

In this study we have demonstrated a clear and measurable effect of tree species richness across various aspects of land-surface phenology in Zambian deciduous savannas. We showed that tree species richness led to an increase in cumulative EVI and season length. Additionally, species richness led to a slower rate of greening and caused the onset of greening to occur earlier with respect to the start of the rainy season. Our study lends support for a positive biodiversity - ecosystem function relationship in our chosen study area, operating through its influence on phenology. Our results exemplify the key role of tree species biodiversity in driving key ecosystem processes, which affect ecosystem structure, the wildlife provisioning role, and the gross primary productivity of ecosystems. Our finding that species richness strongly affects patterns of land-surface phenology in deciduous

savannas has important consequences for two pertinent fields of ecological research. Firstly, it should prompt conservation scientists to take advantage of remotely sensed land-surface phenology data to improve estimates of tree species diversity. The technology behind remote-sensing of tree species diversity is maturing fast, providing a means to rapidly and accurately assess the conservation priority of biodiversity hotspots, and to identify regions suffering biodiversity loss. Secondly, it can provide earth surface system modellers with a means to better understand how future changes in species diversity and composition will affect land-surface phenology and therefore the carbon cycle. Incorporating predictions of biotic change into carbon models has been slow, owing to large uncertainties in the effects of diversity on Gross Primary Productivity (GPP). Our study provides a link by demonstrating a strong positive relationship between species richness and EVI, which itself drives GPP.

Patterns of senescence were poorly predicted by species richness and evenness in our models. Cho et al. (2017) found that tree cover, measured by MODIS LAI data, had a significant effect on senescence rates in savannas in South Africa, which have similar climatic conditions to the sites in our study. In sparse savannas, while the onset of the growing season is often driven by tree photosynthetic activity, which may precede the onset of precipitation, the end of the growing season is conversely driven by the understorey grass layer, which can itself be dependent on tree cover (Cho et al., 2017; Guan et al., 2014). Grass activity is much more reactive to short-term changes in soil moisture than tree activity, and may oscillate within the senescence period. This may explain the lack of a strong precipitation signal for senescence lag and senescence rate. Other studies both global and within southern African savannas have largely ignored patterns of senescence, instead focussing patterns of green-up (Gallinat et al., 2015). Most commonly, these studies simply correlate the decline of rainfall with senescence, but the lack of precipitation as a term in our best model suggests that other unmeasured factors are at play. Alternatively, Zani et al. (2020) suggests that in resource limited environments, senescence times may largely be set by the preceding photosynthetic activity and sink-limitations on growth. For example, limited nutrient supply may prohibit photosynthesis late in the season if the preceding photosynthetic activity has depleted that supply. Reich et al. (1992) suggested that there may be direct constraints on leaf life-span, especially in disturbance and drought-prone environments such as those studied here, which would lead to senescence rate being set largely by the time since bud-burst. In our study however, we found that there was variation in season length between plots, indicating that there are additional factors at play.

While leaf senescence may not be as important for the survival of browsing herbivores as the green-up period, the timing of senescence with respect to temperature and precipitation has important consequences for the savanna understorey microclimate. The longer leaf material remains in the canopy after the end of the rainy season, the greater the microclimatic buffer for herbaceous understorey

279 plants and animals, which require water and protection from high levels of insolation and dry air
280 which can prevail rapidly after the end of the rainy season (Guan et al., 2014). Our study merely
281 exemplifies that more work needs to be done to properly characterise the drivers of senescence in
282 this biome.

283 While species richness is a common measure of biodiversity, abundance evenness constitutes a second
284 key but related axis (Wilsey et al., 2005; Hillebrand et al., 2008; Jost, 2010). In this study, we found
285 contrasting effects of richness and evenness on both cumulative EVI and season length. Evenness
286 caused a decrease in these phenological metrics, which we did not expect. It is possible that the
287 negative effect of abundance evenness occurred because an increase in evenness is associated with a
288 reduction in the canopy cover of a few highly dominant large canopy tree species (e.g. *Brachystegia*
289 *boehmii* and *Julbernardia paniculata*), as part of the transition from woody savanna to thicket
290 vegetation, or following a major disturbance event. Large canopy tree species have access to ground
291 water for a longer part of the year, due to their deep root systems and conservative growth patterns.
292 A future study may choose to explore the differential effects of species diversity in different size
293 classes and in different physiognomic groups defined by functional form, e.g. shrub, canopy tree,
294 coppicing tree.

295 Our coverage of very short season lengths in Zambia, as estimated by the VIPPHEN product,
296 was restricted, with notable absences of plot data in the northeast of the country around 30.5°E,
297 11.5°S, and 23.0°E, 15.0°S. Upon further inspection of true colour satellite imagery, these regions are
298 largely seasonally water-logged floodplain and swampland, and were likely ignored by the ILUA-II
299 assessment for this reason. This also explains their divergent phenological patterns as observed in
300 the MODIS EVI data.

301 It is important to note that the remotely sensed EVI measurements used here aren't specific only
302 to trees, they represent the landscape as a single unit. Nevertheless, seasonal patterns of tree leaf
303 phenology in southern African deciduous woodlands, particularly the pre-rainy season green-up phe-
304 nomenon, is driven almost exclusively by trees, while grasses tend to follow patterns of precipitation
305 more closely (Whitecross et al., 2017; Archibald & Scholes, 2007; Higgins et al., 2011). Grasses con-
306 tribute to gross primary productivity, and it was therefore in our interests to include their response in
307 our analysis as we seek to demonstrate how tree species richness can affect cycles of carbon exchange.
308 Additionally, the micro-climatic effects of tree leaf canopy coverage and hydraulic lift through tree
309 deep root systems will benefit the productivity of grasses as well as understorey tree individuals.

310 It is possible that not all tree individuals in our dataset exhibited a completely deciduous growth
311 pattern. Some highly conservative species in this region remain evergreen throughout the dry season.

5 Conclusion

Here we explored the role of tree species diversity on land surface phenology across Zambia. We showed that species richness clearly affects rate of green-up, the lag time between rainy season onset and growth, and the length of the growing season. Our results have a range of consequences for earth system modellers and conservation managers, and lend further support to an already well established corpus of the positive effect of species diversity on ecosystem function.

References

- Adole, T., J. Dash & P. M. Atkinson (2018a). “Characterising the land surface phenology of Africa using 500 m MODIS EVI”. In: *Applied Geography* 90, pp. 187–199. DOI: 10.1016/j.apgeog.2017.12.006.
- Adole, T., J. Dash & P. M. Atkinson (2018b). “Large-scale prerain vegetation green-up across Africa”. In: *Global Change Biology* 24.9, pp. 4054–4068. DOI: 10.1111/gcb.14310.
- Araujo, H. F. P. de, A. H. Vieira-Filho, M. R. V. Barbosa, J. A. F. Diniz-Filho & J. M. C. da Silva (2017). “Passerine phenology in the largest tropical dry forest of South America: Effects of climate and resource availability”. In: *Emu - Austral Ornithology* 117.1, pp. 78–91. DOI: 10.1080/01584197.2016.1265430.
- Archibald, S. & R. J. Scholes (2007). “Leaf green-up in a semi-arid African savanna -separating tree and grass responses to environmental cues”. In: *Journal of Vegetation Science* 18.4, pp. 583–594. DOI: 10.1111/j.1654-1103.2007.tb02572.x.
- Bale, J. S., G. J. Masters, I. D. Hodkinson, C. Awmack, T. M. Bezemer, V. K. Brown, J. Butterfield, A. Buse, J. C. Coulson, J. Farrar, et al. (2002). “Herbivory in global climate change research: direct effects of rising temperature on insect herbivores”. In: *Global Change Biology* 8.1, pp. 1–16. DOI: 10.1046/j.1365-2486.2002.00451.x.
- Bloom, A. A., J. Exbrayat, I. R. van der Velde, L. Feng & M. Williams (2016). “The decadal state of the terrestrial carbon cycle: Global retrievals of terrestrial carbon allocation, pools, and residence times”. In: *Proceedings of the National Academy of Sciences* 113.5, pp. 1285–1290. DOI: 10.1073/pnas.1515160113.
- Broadhead, J. S., C. K. Ong & C. R. Black (2003). “Tree phenology and water availability in semi-arid agroforestry systems”. In: *Forest Ecology and Management* 180.1-3, pp. 61–73. DOI: 10.1016/s0378-1127(02)00602-3.
- Chidumayo, E. N. (2001). “Climate and phenology of savanna vegetation in southern Africa”. In: *Journal of Vegetation Science* 12.3, p. 347. DOI: 10.2307/3236848.

344 Cho, M. A., A. Ramoelo & L. Dziba (2017). “Response of land surface phenology to variation in
345 tree cover during green-up and senescence periods in the semi-arid savanna of southern Africa”.
346 In: *Remote Sensing* 9.7, p. 689. DOI: 10.3390/rs9070689.

347 Cole, E. F., P. R. Long, P. Zelazowski, M. Szulkin & B. C. Sheldon (2015). “Predicting bird phenology
348 from space: Satellite-derived vegetation green-up signal uncovers spatial variation in phenological
349 synchrony between birds and their environment”. In: *Ecology and Evolution* 5.21, pp. 5057–5074.
350 DOI: 10.1002/ece3.1745.

351 Curtis, R. O. & D. D. Marshall (2000). “Technical Note: Why Quadratic Mean Diameter?” In: 15.3,
352 pp. 137–139. DOI: 10.1093/wjaf/15.3.137.

353 Dahlin, K. M., D. Del Ponte, E. Setlock & R. Nagelkirk (2016). “Global patterns of drought deciduous
354 phenology in semi-arid and savanna-type ecosystems”. In: *Ecography* 40.2, pp. 314–323. DOI: 10.
355 1111/ecog.02443.

356 Didan, L. (2015). *MOD13Q1 MODIS/Terra Vegetation Indices 16-Day L3 Global 250m SIN Grid*
357 *V006 [Data set]*. NASA EOSDIS Land Processes DAAC. DOI: 10.5067/MODIS/MOD13Q1.006.
358 (Visited on 08/05/2020).

359 Didan, L. & A. Barreto (2016). *NASA MEaSUREs Vegetation Index and Phenology (VIP) Phenology*
360 *EVI2 Yearly Global 0.05Deg CMG [Data set]*. NASA EOSDIS Land Processes DAAC. DOI: 10.
361 5067/MEaSUREs/VIP/VIPPHEN_EVI2.004. (Visited on 08/05/2020).

362 Dinerstein, E., D. Olson, A. Joshi, C. Vynne, N. D. Burgess, E. Wikramanayake, N. Hahn, S.
363 Palminteri, P. Hedao, R. Noss, et al. (2017). “An ecoregion-based approach to protecting half the
364 terrestrial realm”. In: *BioScience* 67.6, pp. 534–545. DOI: 10.1093/biosci/bix014.

365 Dufrêne, M. & P. Legendre (1997). “Species assemblage and indicator species: The need for a flex-
366 ible asymmetrical approach”. In: *Ecological Monographs* 67, pp. 345–366. DOI: 10.1890/0012-
367 9615(1997)067[0345:SAAIST]2.0.CO;2.

368 Fayolle, A., M. D. Swaine, J. Bastin, N. Bourland, J. A. Comiskey, G. Dauby, J. Doucet, J. Gillet,
369 S. Gourlet-Fleury, O. J. Hardy, et al. (2014). “Patterns of tree species composition across tropical
370 African forests”. In: *Journal of Biogeography* 41.12, pp. 2320–2331. DOI: 10.1111/jbi.12382.

371 Fick, S. E. & R. J. Hijmans (2017). “WorldClim 2: New 1-km spatial resolution climate surfaces for
372 global land areas”. In: *International Journal of Climatology* 37.12, pp. 4302–4315. DOI: 10.1002/
373 joc.5086.

374 Fuller, D. O. (1999). “Canopy phenology of some mopane and miombo woodlands in eastern Zambia”.
375 In: *Global Ecology and Biogeography* 8.3-4, pp. 199–209. DOI: 10.1046/j.1365-2699.1999.00130.
376 x.

377 Gallinat, A. S., R. B. Primack & D. L. Wagner (2015). “Autumn, the neglected season in climate
378 change research”. In: 30.3, pp. 169–176. DOI: 10.1016/j.tree.2015.01.004.

379 Gu, L., W. M. Post, D. Baldocchi, T. A. Black, S. B. Verma, T. Vesala & S. C. Wofsy (2003).
 380 “Phenology of vegetation photosynthesis”. In: *Phenology: An Integrative Environmental Science*.
 381 Springer Netherlands, pp. 467–485. DOI: 10.1007/978-94-007-0632-3_29.
 382 Guan, K., E. F. Wood, D. Medvigy, J. Kimball, M. Pan, K. K. Caylor, J. Sheffield, C. Xu & M. O.
 383 Jones (2014). “Terrestrial hydrological controls on land surface phenology of African savannas
 384 and woodlands”. In: *Journal of Geophysical Research: Biogeosciences* 119.8, pp. 1652–1669. DOI:
 385 10.1002/2013jg002572.
 386 Higgins, S. I., M. D. Delgado-Cartay, E. C. February & H. J. Combrink (2011). “Is there a temporal
 387 niche separation in the leaf phenology of savanna trees and grasses?” In: *Journal of Biogeography*
 388 38.11, pp. 2165–2175. DOI: 10.1111/j.1365-2699.2011.02549.x.
 389 Hillebrand, H., D. M. Bennett & M. W. Cadotte (2008). “Consequences of dominance: A review of
 390 evenness effects on local and regional ecosystem processes”. In: *Ecology* 89.6, pp. 1510–1520. DOI:
 391 10.1890/07-1053.1.
 392 Huffman, G. J., E. F. Stocker, D. Bolvin, E. J. Nelkin & J. Tan (2015). *GPM IMERG Final Precipita-*
 393 *tion L3 1 day 0.1 degree x 0.1 degree V06 [Data set]*. Goddard Earth Sciences Data and Information
 394 Services Center (GES DISC). DOI: 10.5067/MODIS/MOD13Q1.006. (Visited on 10/30/2020).
 395 Jeganathan, C., J. Dash & P. M. Atkinson (2014). “Remotely sensed trends in the phenology of
 396 northern high latitude terrestrial vegetation, controlling for land cover change and vegetation
 397 type”. In: *Remote Sensing of Environment* 143, pp. 154–170. DOI: 10.1016/j.rse.2013.11.020.
 398 Jost, L. (2007). “Partitioning diversity into independent alpha and beta components”. In: *Ecology*
 399 88.10, pp. 2427–2439. DOI: 10.1890/06-1736.1.
 400 Jost, L. (2010). “The relation between evenness and diversity”. In: *Diversity* 2.2, pp. 207–232. DOI:
 401 10.3390/d2020207.
 402 Kreft, H. & W. Jetz (2010). “A framework for delineating biogeographical regions based on species
 403 distributions”. In: *Journal of Biogeography* 37.11, pp. 2029–2053. DOI: 10.1111/j.1365-2699.
 404 2010.02375.x.
 405 Lüdecke, D. (2018). “ggeffects: Tidy data frames of marginal effects from regression models.” In:
 406 *Journal of Open Source Software* 3.26, p. 772. DOI: 10.21105/joss.00772.
 407 Morellato, L. P. C., B. Alberton, S. T. Alvarado, B. Borges, E. Buisson, M. G. G. Camargo, L. F.
 408 Cancian, D. W. Carstensen, D. F. E. Escobar, P. T. P. Leite, et al. (2016). “Linking plant phenology
 409 to conservation biology”. In: *Biological Conservation* 195, pp. 60–72. DOI: 10.1016/j.biocon.
 410 2015.12.033.
 411 Mukosha, J. & A. Siampale (2009). *Integrated land use assessment Zambia 2005–2008*. Lusaka,
 412 Zambia: Ministry of Tourism, Environment et al.

413 Murtagh, F. & P. Legendre (2014). “Ward’s hierarchical agglomerative clustering method: Which
 414 algorithms implement Ward’s criterion?” In: *Journal of Classification* 31.3, pp. 274–295. DOI:
 415 10.1007/s00357-014-9161-z.

416 Ogutu, J. O., H. Piepho & H. T. Dublin (2013). “Responses of phenology, synchrony and fecundity
 417 of breeding by African ungulates to interannual variation in rainfall”. In: *Wildlife Research* 40.8,
 418 p. 698. DOI: 10.1071/wr13117.

419 Parr, C. L., C. E. R. Lehmann, W. J. Bond, W. A. Hoffmann & A. N. Andersen (2014). “Tropical
 420 grassy biomes: Misunderstood, neglected, and under threat”. In: *Trends in Ecology and Evolution*
 421 29, pp. 205–213. DOI: 10.1016/j.tree.2014.02.004.

422 Pavlick, R., D. T. Drewry, K. Bohn, B. Reu & A. Kleidon (2013). “The Jena Diversity-Dynamic
 423 Global Vegetation Model (JeDi-DGVM): A diverse approach to representing terrestrial biogeogra-
 424 phy and biogeochemistry based on plant functional trade-offs”. In: *Biogeosciences* 10.6, pp. 4137–
 425 4177. DOI: 10.5194/bg-10-4137-2013.

426 Pelletier, J., A. Paquette, K. Mbindo, N. Zimba, A. Siampale, B. Chendauka, F. Siangulube & J. W.
 427 Roberts (2018). “Carbon sink despite large deforestation in African tropical dry forests (miombo
 428 woodlands)”. In: *Environmental Research Letters* 13, p. 094017. DOI: 10.1088/1748-9326/aadc9a.

429 Penuelas, J., T. Rutishauser & I. Filella (2009). “Phenology feedbacks on climate change”. In: *Science*
 430 324.5929, pp. 887–888. DOI: 10.1126/science.1173004.

431 Prather, C. M., S. L. Pelini, A. Laws, E. Rivest, M. Woltz, C. P. Bloch, I. Del Toro, C. Ho, J.
 432 Kominoski, T. A. S. Newbold, et al. (2012). “Invertebrates, ecosystem services and climate change”.
 433 In: *Biological Reviews* 88.2, pp. 327–348. DOI: 10.1111/brv.12002.

434 R Core Team (2020). *R: A Language and Environment for Statistical Computing*. R Foundation for
 435 Statistical Computing. Vienna, Austria. URL: <https://www.R-project.org/>.

436 Reich, P. B., M. B. Walters & D. S. Ellsworth (1992). “Leaf life-span in relation to leaf, plant, and
 437 stand characteristics among diverse ecosystems”. In: 62.3, pp. 365–392. DOI: 10.2307/2937116.

438 Richardson, A. D., T. F. Keenan, M. Migliavacca, Y. Ryu, O. Sonnentag & M. Toomey (2013). “Cli-
 439 mate change, phenology, and phenological control of vegetation feedbacks to the climate system”.
 440 In: *Agricultural and Forest Meteorology* 169, pp. 156–173. DOI: 10.1016/j.agrformet.2012.09.
 441 012.

442 Rousseeuw, P. J. (1987). “Silhouettes: A graphical aid to the interpretation and validation of cluster
 443 analysis”. In: *Journal of Computational and Applied Mathematics* 20, pp. 53–65. DOI: 10.1016/
 444 0377-0427(87)90125-7.

445 Ryan, C. M., M. Williams, J. Grace, E. Woollen & C. E. R. Lehmann (2017). “Pre-rain green-up is
 446 ubiquitous across southern tropical Africa: implications for temporal niche separation and model
 447 representation”. In: *New Phytologist* 213.2, pp. 625–633. DOI: 10.1111/nph.14262.

448 Scheiter, S., L. Langan & S. I. Higgins (2013). “Next-generation dynamic global vegetation models:
 449 Learning from community ecology”. In: *New Phytologist* 198.3, pp. 957–969. DOI: 10.1111/nph.
 450 12210.

451 Sjöström, M., J. Ardö, A. Arneth, N. Boulain, B. Cappelaere, L. Eklundh, A. de Grandcourt, W. L.
 452 Kutsch, L. Merbold & Y. Nouvellon (2011). “Exploring the potential of MODIS EVI for modeling
 453 gross primary production across African ecosystems”. In: *Remote Sensing of Environment* 115.4,
 454 pp. 1081–1089. DOI: 10.1016/j.rse.2010.12.013.

455 Smith, B. & J. B. Wilson (1996). “A consumer’s guide to evenness indices”. In: *Oikos* 76, pp. 70–82.
 456 DOI: 10.2307/3545749.

457 Stan, K. & A. Sanchez-Azofeifa (2019). “Tropical dry forest diversity, climatic response, and resilience
 458 in a changing climate”. In: *Forests* 10.5, p. 443. DOI: 10.3390/f10050443.

459 Stöckli, R., T. Rutishauser, I. Baker, M. A. Liniger & A. S. Denning (2011). “A global reanalysis of
 460 vegetation phenology”. In: *Journal of Geophysical Research* 116.G3. DOI: 10.1029/2010jg001545.

461 Velasque, M. & K. Del-Claro (2016). “Host plant phenology may determine the abundance of an
 462 ecosystem engineering herbivore in a tropical savanna”. In: *Ecological Entomology* 41.4, pp. 421–
 463 430. DOI: 10.1111/een.12317.

464 White, M. A., K. M. de Beurs, K. Didan, D. W. Inouye, A. D. Richardson, O. P. Jensen, J. O’Keefe,
 465 G. Zhang, R. R. Nemani, W. J. D. Van Leeuwen, et al. (2009). “Intercomparison, interpretation,
 466 and assessment of spring phenology in North America estimated from remote sensing for 1982–
 467 2006”. In: *Global Change Biology* 15.10, pp. 2335–2359. DOI: 10.1111/j.1365-2486.2009.01910.
 468 x.

469 Whitecross, M. A., E. T. F. Witkowski & S. Archibald (2017). “Savanna tree-grass interactions:
 470 A phenological investigation of green-up in relation to water availability over three seasons”. In:
 471 *South African Journal of Botany* 108, pp. 29–40. DOI: 10.1016/j.sajb.2016.09.003.

472 Whitley, R., J. Beringer, L. B. Hutley, G. Abramowitz, M. G. De Kauwe, B. Evans, V. Haverd, L.
 473 Li, C. Moore, Y. Ryu, et al. (2017). “Challenges and opportunities in land surface modelling of
 474 savanna ecosystems”. In: *Biogeosciences* 14.20, pp. 4711–4732. DOI: 10.5194/bg-14-4711-2017.

475 Wilsey, B. J., D. R. Chalcraft, C. M. Bowles & M. R. Willig (2005). “Relationships among indices
 476 suggest that richness is an incomplete surrogate for grassland biodiversity”. In: *Ecology* 86.5,
 477 pp. 1178–1184. DOI: 10.1890/04-0394.

478 Xia, J., S. Niu, P. Ciais, I. A. Janssens, J. Chen, C. Ammann, A. Arain, P. D. Blanken, A. Cescatti,
 479 D. Bonal, et al. (2015). “Joint control of terrestrial gross primary productivity by plant phenology
 480 and physiology”. In: *Proceedings of the National Academy of Sciences* 112.9, pp. 2788–2793. DOI:
 481 10.1073/pnas.1413090112.

482 Zani, D., T. W. Crowther, L. Mo, S. S. Renner & C. M. Zohner (2020). “Increased growing-season
483 productivity drives earlier autumn leaf senescence in temperate trees”. In: 370.6520, pp. 1066–
484 1071. DOI: 10.1126/science.abd8911.

485 Zuur, A., E. N. Ieno, N. Walker, A. A. Saveliev & G. M. Smith (2009). *Mixed effects models and*
486 *extensions in ecology with R*. New York NY, USA: Springer.

487 6 Supplementary Material

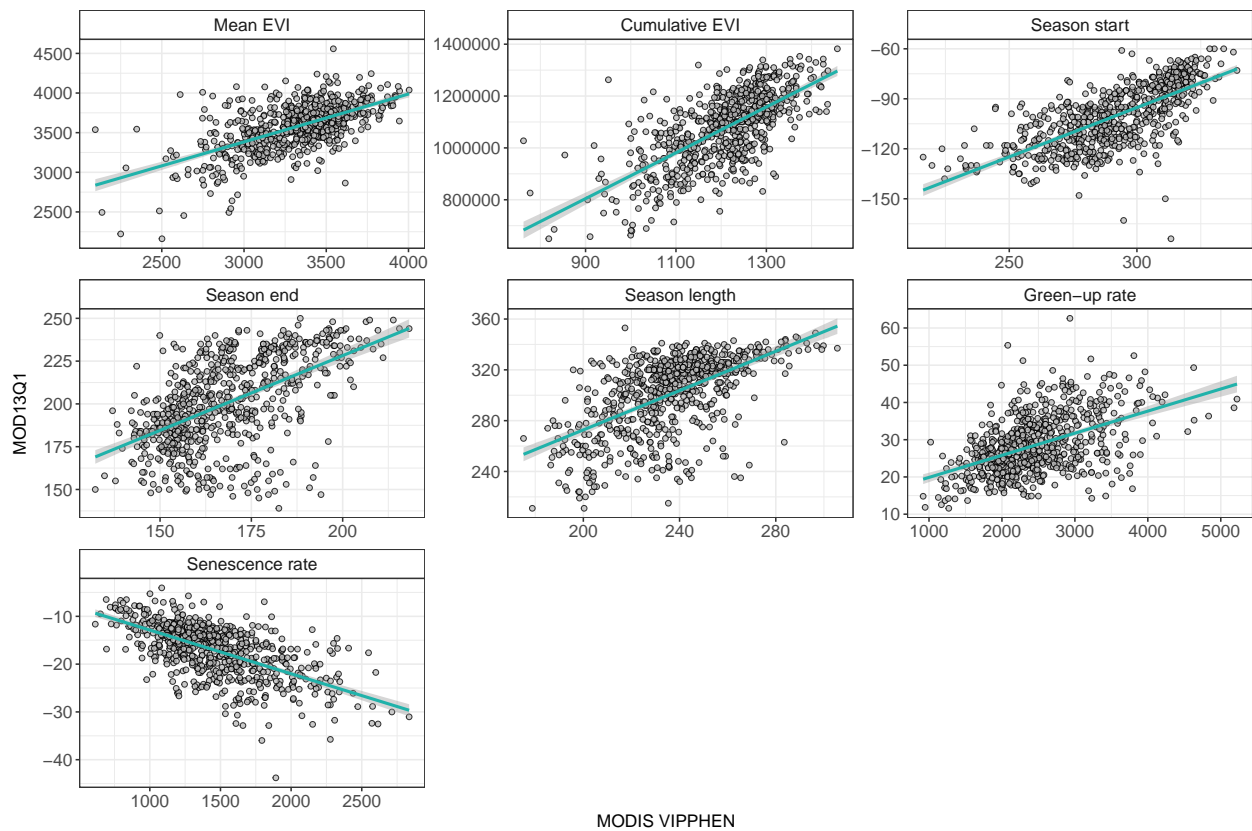


Figure S1: Scatter plots showing a comparison of phenological metrics from the MODIS VIPPHEN product (Didan & Barreto, 2016) and those extracted from the MOD13Q1 data (Didan, 2015), for each of the sites in our study. The cyan line shows a linear model of the data, with a 95% confidence interval.

Response	DoF	F	Prob.	R ²
Mean EVI	672	387.0	p<0.05	0.37
Cumulative EVI	672	592.6	p<0.05	0.47
Season start	672	660.3	p<0.05	0.50
Season end	672	285.0	p<0.05	0.30
Season length	672	325.0	p<0.05	0.33
Green-up rate	672	217.2	p<0.05	0.24
Senescence rate	672	412.3	p<0.05	0.38

Table S1: Model fit statistics for comparison of MODIS VIPPHEN and MOD13Q1 products across each of our study sites.

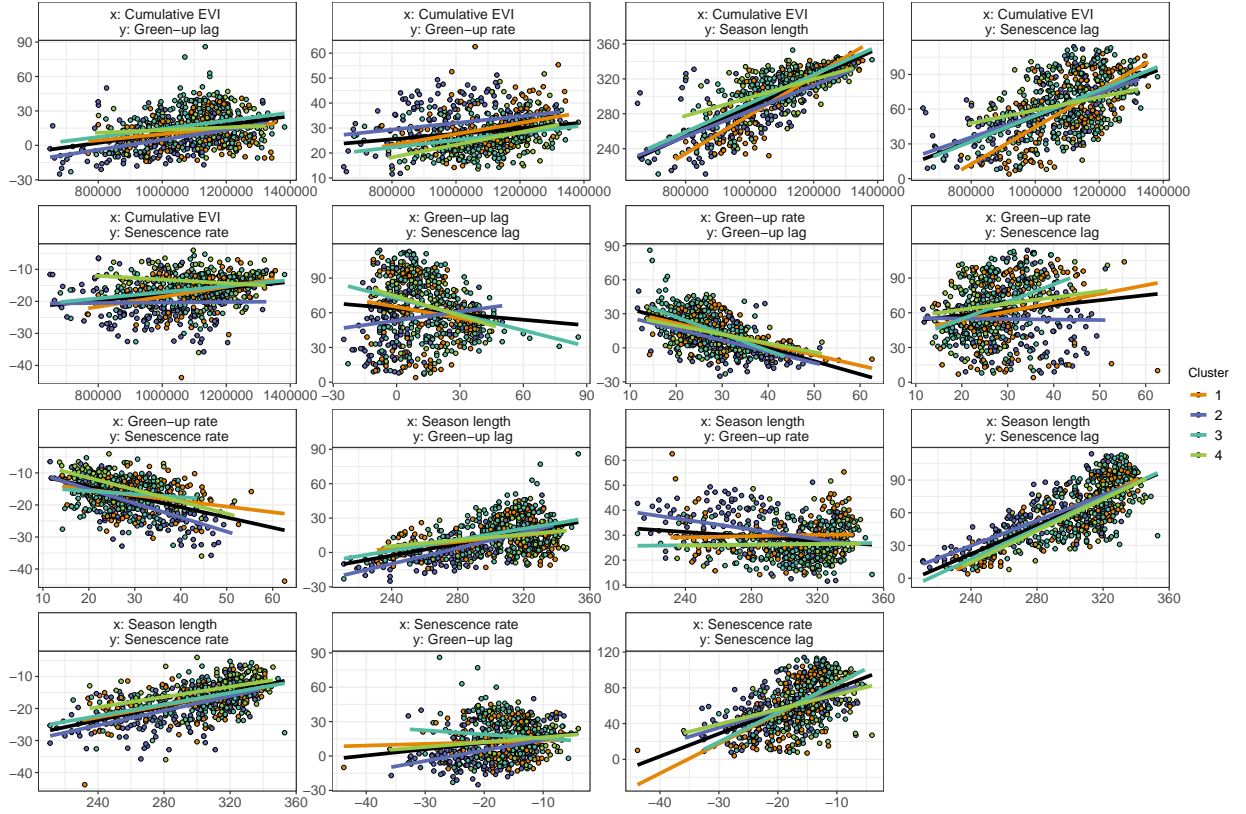


Figure S2: Scatter plots showing pairwise comparisons of the six phenological metrics used in this study, extracted from the MODIS MOD13Q1 product (Didan, 2015). Points represent study sites and are coloured by vegetation type. Linear regression line of best fit for all sites is shown as a black line, while linear regressions are shown for each vegetation type cluster as coloured lines.

Rank	Precipitation	Diurnal dT	Evenness	Richness	Richness:Cluster	logLik	AIC	ΔIC	W_i
1	✓		✓	✓	✓	-8787	17591	0	0.663
2	✓	✓	✓	✓	✓	-8786	17593	1	0.337
<u>3</u>	<u>✓</u>		<u>✓</u>		<u>✓</u>	<u>-8798</u>	<u>17612</u>	<u>20</u>	<u>0.000</u>
4	✓	✓	✓		✓	-8798	17613	22	0.000
5	✓		✓	✓		-8802	17616	25	0.000
6	✓	✓	✓	✓		-8802	17617	26	0.000
7	✓			✓		-8805	17621	30	0.000
8	✓	✓		✓		-8805	17622	31	0.000
9	✓					-8812	17632	41	0.000
10	✓	✓				-8812	17634	42	0.000

Table S2: Cumulative EVI Model selection candidate models, with fit statistics. The overall best model is marked by bold text, while the best model with a richness:cluster interaction term is marked by underlined text

Rank	Precipitation	Diurnal dT	Evenness	Richness	Richness:Cluster	logLik	AIC	ΔIC	W_i
1	✓	✓	✓	✓	✓	-3189	6398	0	0.654
2	✓		✓	✓	✓	-3191	6399	1	0.345
3	✓	✓	✓		✓	-3197	6412	14	0.001
<u>4</u>	<u>✓</u>		<u>✓</u>		<u>✓</u>	<u>-3198</u>	<u>6413</u>	<u>15</u>	<u>0.000</u>
5	✓	✓	✓	✓		-3203	6421	23	0.000
6	✓		✓	✓		-3205	6422	24	0.000
7	✓	✓		✓		-3207	6426	27	0.000
8	✓			✓		-3208	6426	28	0.000
9	✓	✓				-3211	6431	33	0.000
10	✓					-3212	6433	35	0.000

Table S3: Season length Model selection candidate models, with fit statistics. The overall best model is marked by bold text, while the best model with a richness:cluster interaction term is marked by underlined text

Rank	Precipitation	Diurnal dT	Evenness	Richness	Richness:Cluster	logLik	AIC	ΔIC	W_i
1		✓	✓	✓	✓	-2288	4594	0	0.274
2		✓	✓		✓	-2289	4595	1	0.171
3	✓	✓	✓	✓	✓	-2288	4595	2	0.121
4		✓				-2294	4596	2	0.091
5		✓		✓		-2293	4596	2	0.087
<u>6</u>	<u>✓</u>	<u>✓</u>	<u>✓</u>		<u>✓</u>	<u>-2289</u>	<u>4597</u>	<u>3</u>	<u>0.070</u>
7		✓	✓	✓		-2293	4597	4	0.046
8	✓	✓				-2294	4598	4	0.037
9	✓	✓		✓		-2293	4598	4	0.035
10		✓	✓			-2294	4598	4	0.035

Table S4: Green-up rate Model selection candidate models, with fit statistics. The overall best model is marked by bold text, while the best model with a richness:cluster interaction term is marked by underlined text

Rank	Precipitation	Diurnal dT	Evenness	Richness	Richness:Cluster	logLik	AIC	ΔIC	W_i
<u>1</u>		<u>✓</u>	<u>✓</u>	<u>✓</u>	<u>✓</u>	-2091	4200	0	0.320
2	✓	✓	✓	✓	✓	-2090	4201	1	0.224
3	✓		✓	✓	✓	-2092	4202	2	0.139
4			✓	✓	✓	-2093	4202	2	0.105
5		✓	✓		✓	-2094	4204	4	0.039
6		✓	✓	✓		-2096	4205	5	0.026
7		✓		✓		-2098	4206	6	0.019
8	✓	✓	✓	✓		-2096	4206	6	0.019
9	✓	✓	✓		✓	-2094	4206	6	0.019
10			✓		✓	-2096	4206	6	0.017

Table S5: Senescence rate Model selection candidate models, with fit statistics. The overall best model is marked by bold text, while the best model with a richness:cluster interaction term is marked by underlined text

Rank	Precipitation	Diurnal dT	Evenness	Richness	Richness:Cluster	logLik	AIC	ΔIC	W_i
1	✓	✓	✓	✓	✓	-2704	5429	0	0.957
2	✓	✓	✓	✓		-2711	5435	6	0.043
<u>3</u>		<u>✓</u>	<u>✓</u>	<u>✓</u>	<u>✓</u>	<u>-2727</u>	<u>5472</u>	<u>43</u>	<u>0.000</u>
4		✓	✓	✓		-2734	5479	50	0.000
5	✓	✓	✓		✓	-2733	5484	55	0.000
6	✓	✓	✓			-2737	5486	57	0.000
7	✓	✓		✓		-2742	5497	68	0.000
8	✓	✓				-2746	5501	72	0.000
9		✓	✓		✓	-2758	5532	103	0.000
10		✓	✓			-2762	5534	105	0.000

Table S6: Green-up lag Model selection candidate models, with fit statistics. The overall best model is marked by bold text, while the best model with a richness:cluster interaction term is marked by underlined text

Rank	Precipitation	Diurnal dT	Evenness	Richness	Richness:Cluster	logLik	AIC	ΔIC	W_i
1		✓	✓		✓	-3106	6228	0	0.492
2		✓	✓	✓	✓	-3106	6229	2	0.230
3	✓	✓	✓		✓	-3106	6230	2	0.183
4	✓	✓	✓	✓	✓	-3106	6231	3	0.087
<u>5</u>		<u>✓</u>		<u>✓</u>		<u>-3115</u>	<u>6239</u>	<u>11</u>	<u>0.002</u>
6		✓				-3116	6239	11	0.002
7		✓	✓			-3115	6239	12	0.001
8		✓	✓	✓		-3114	6241	13	0.001
9	✓	✓				-3115	6241	13	0.001
10	✓	✓		✓		-3114	6241	13	0.001

Table S7: Senescence lag Model selection candidate models, with fit statistics. The overall best model is marked by bold text, while the best model with a richness:cluster interaction term is marked by underlined text

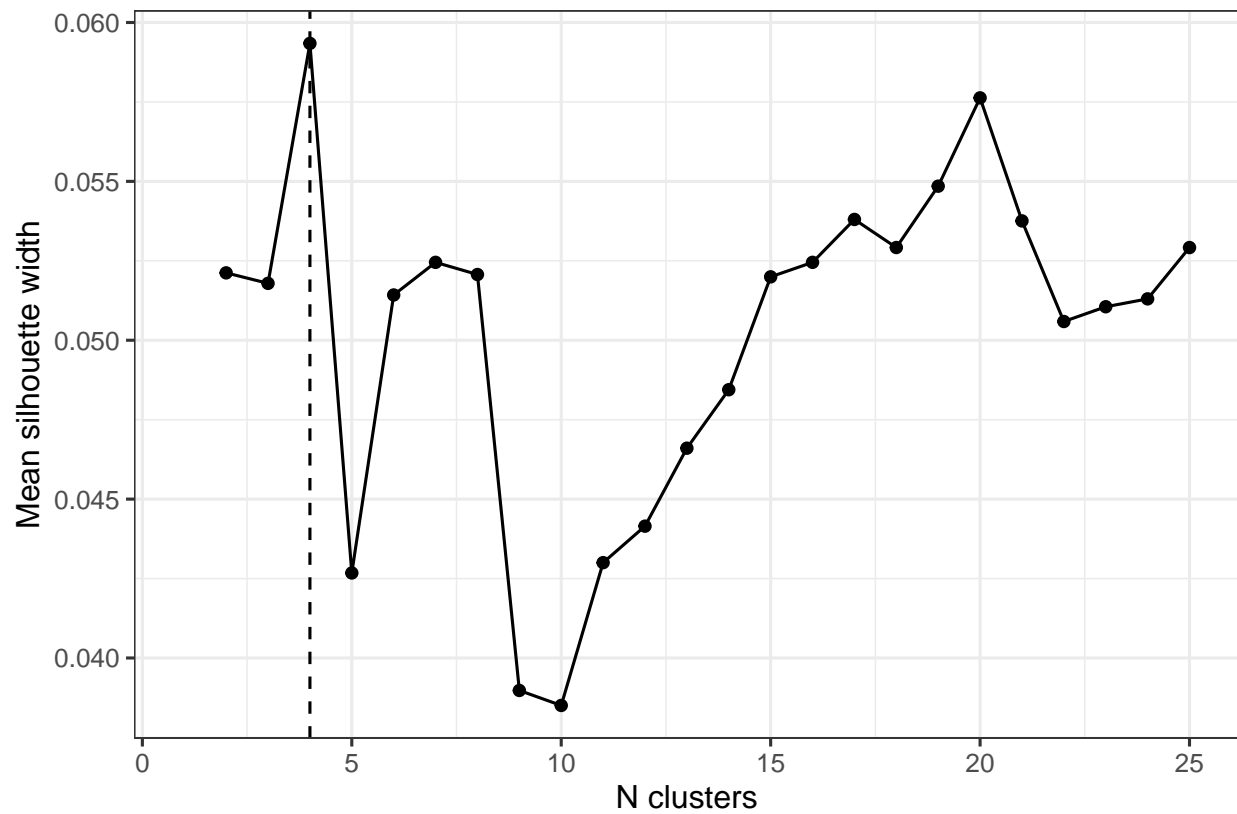


Figure S3: Mean silhouette width for agglomerative hierarchical clustering, specifying a varying number of clusters. The highest silhouette width, and therefore the number of clusters chosen in our analysis, is denoted by a dashed line.

Response	Clusters	Estimate	SE	DoF	T ratio	Prob.
Cumulative EVI	1-2	1.1E-14	6.68E-14	697	0.17	0.98
	1-3	5.5E-14	6.33E-14	697	0.87	0.66
	2-3	4.4E-14	8.16E-14	697	0.54	0.85
Season length	1-2	-6.4E-18	1.56E-17	698	-0.41	0.91
	1-3	1.9E-17	1.48E-17	698	1.26	0.42
	2-3	2.5E-17	1.89E-17	698	1.32	0.38
Green-up rate	1-2	1.1E-18	4.89E-18	698	0.23	0.97
	1-3	-3.5E-18	4.59E-18	698	-0.76	0.73
	2-3	-4.6E-18	5.91E-18	698	-0.78	0.72
Senescence rate	1-2	3.7E-18	3.41E-18	698	1.09	0.52
	1-3	6.3E-18	3.21E-18	698	1.97	0.12
	2-3	2.6E-18	4.14E-18	698	0.63	0.80
Green-up lag	1-2	-7.3E-18	1.03E-17	698	-0.71	0.76
	1-3	6.0E-18	9.71E-18	698	0.62	0.81
	2-3	1.3E-17	1.25E-17	698	1.07	0.54
Senescence lag	1-2	2.9E-19	1.30E-17	698	0.02	1.00
	1-3	6.1E-18	1.23E-17	698	0.50	0.87
	2-3	5.9E-18	1.59E-17	698	0.37	0.93

Table S8: Comparisons of interaction marginal effects using post-hoc Tukey's tests.